Charge-Transfer Dynamics at Model Metal−Organic Solar Cell Surfaces

J. Ben Taylor,[†] Louise C. Mayor,[†] Janine C. Swarbrick,[†] James N. O'Shea,*[,†] and Joachim Schnadt[‡]

School of Physics and Astronomy, University of Nottingham, University Park, Nottingham, NG7 2RD, United Kingdom, and Department of Synchrotron Radiation Research, Lund University, P.O. Box 117, S-221 00 Lund, Sweden

Received: July 10, 2007; In Final Form: August 21, 2007

The "core-hole clock" implementation of resonant photoemission has been used to investigate the charge-transfer dynamics of bi-isonicotinic acid molecules (4,4′-dicarboxy-2,2′-bipyridine) adsorbed on a rutile TiO_2-(110) surface containing varying densities of gold islands. In the presence of, nominally, a few monolayers of gold there exists a strong coupling between the adsorbed molecules and the surface. This is derived from the measurement of a <3 fs charge-transfer time for the injection of a core-excited electron into the substrate. This ultrafast charge-transfer time is quenched for a fraction of the molecules upon the addition of only a few further monolayers of gold. There is evidence to suggest that this effect derives from a change in the bonding configuration of bi-isonicotinic acid molecules. However, results also support the occurrence of ultrafast back-transfer from Au states to core-excited unoccupied molecular states.

1. Introduction

In principle, solar cells offer an extremely attractive solution to the need for clean energy. The Earth receives $\sim 3 \times 10^{24}$ J of solar energy per year, orders of magnitude more energy than is consumed worldwide.[1] However, the use of photovoltaics has been limited by the costly materials and fabrication of the conventional solid-state devices that were the first to emerge. This problem is beginning to be overcome by the development of a new class of cells, namely organic photovoltaics (OPV). Such devices use relatively cheap substrates and organic overlayers, often with the additional advantage of tunable structural and aesthetic properties.

One of the most efficient devices is the Grätzel cell.[2,3] It operates on the principle of sensitizing a film of interconnected TiO_2 colloids with dye molecules such as "N3" ($(dcb)_2Ru(NCS)_2$, where dcb stands for 4,4′-dicarboxy-2,2′-bipyridine). This system is then placed in contact with an electrolyte. Electrons in the highest occupied molecular orbitals (HOMO) of the dye absorb photons and are promoted into the lowest unoccupied molecular orbitals (LUMO), which reside above the substrate band gap. These electrons are then injected into the semiconductor conduction band where they move to the counter electrode of the system. Replenishment of electrons in the oxidized dye molecules comes from the reduced species of the redox couple present in the electrolyte; replenishment of the reduced species occurs at the counter electrode that is also in contact with the electrolyte. Such cells are currently being manufactured and offer a credible alternative to inorganic devices. They fall under the OPV subclass of dye-sensitized solar cells (DSSC).

A relatively new DSSC that shows promise is that developed by McFarland and Tang.[4] Their cell consists of the four layers, dye/Au/TiO_2/Ti. It was proposed that, following photoexcitation of the dye, electrons are injected from molecular orbitals residing above the Schottky barrier into the TiO_2 layer via ballistic passage through an ultrathin Au film that ranges in thickness from 15−50 nm. The Au layer then scavenges the holes left behind in the dye molecules. In this way, the cell is simplified in comparison to other DSSCs, having no need of an electrolyte. A photovoltage is formed by contact between the Au film and the Ti back-plate. A merbromin dye on a Au/TiO_2/Ti multilayer was found to give an open-circuit voltage of 600−800 mV and a short-circuit current of 10−18 μA cm^{-2} at an efficiency of $<1\%$. Although this is low, it was also found that 10% of the adsorbed photons gave rise to an electric current.[4,5] This relatively high internal quantum efficiency makes the cell and the associated interfaces of great interest.

The exact nature of the interfaces of this cell and the roles of the interactions therein are still under investigation. The explanation of ballistic passage is highly plausible on the basis of electron mean-free-paths through noble metal films of comparable thickness.[6] However, there is also the possibility of energy transferring from the dye to excite Au electrons, which are subsequently injected into the conduction band of the semiconductor.[5] Furthermore, the interfaces are not strictly as linear as their denotation of dye/Au/TiO_2 would suggest. On TiO_2, in the case of deposition by sublimation[7−9] and sputtering,[10] Au grows as islands. It has been shown[10] that a significant fraction of TiO_2(110) surface is still exposed following deposition of a Au film with a nominal thickness of 30 nm. Dye molecules may therefore interact simultaneously with the Au islands/network and the TiO_2 substrate.

In the continuing investigation of the McFarland and Tang model system, this report presents the interfacial study of bi-isonicotinic acid (4,4′-dicarboxy-2,2′-bipyridine) adsorbed on gold-covered rutile TiO_2(110). The motivation for using bi-isonicotinic acid is that it is the ligand through which a variety of dye molecules, most notably N3, are chemically bound to the TiO_2 surface in Grätzel DSSCs. The study of bi-isonicotinic acid thus gives a measure of how such technologically important

* To whom correspondence should be addressed. E-mail: james.oshea@nottingham.ac.uk

[†] University of Nottingham.

[‡] Lund University.

10.1021/jp075366d CCC: $37.00
Published on Web 10/04/2007

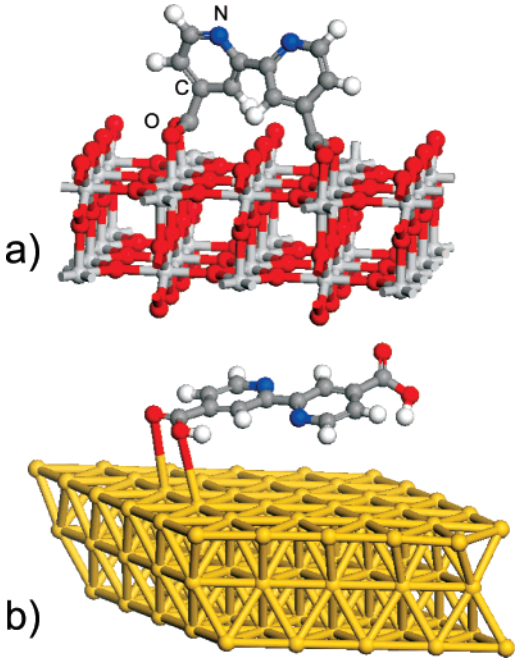

Figure 1. Schematic illustration of the adsorption geometry of bi-isonicotinic acid on (a) TiO_2(110) in a 2M-bidendate fashion via the deprotanated carboxylic groups[11,12] and (b) Au(111) largely parallel to the surface with bonding through one or more intact carboxylic groups.[18]

dyes will anchor. The advantage of using the ligand as opposed to the full dye is that it is stable to sublimation, allowing in situ ultrahigh vacuum (UHV) preparation of the sample. In addition, a large number of studies have also been carried out for the molecule[11−18] on related surfaces, which we draw on here in our interpretation of this relatively complex system. The molecular structure of bi-isonicotinic acid and its adsorption geometry on the surfaces of TiO_2(110) and Au(111) deduced from these studies are schematically shown in Figure 1.

2. Method

The experiments were carried out at the Swedish synchrotron facility MAX-lab in Lund. Beamline I311[19] was used, which has a photon energy range of 30−1500 eV and is equipped with a Scienta SES200 hemispherical analyzer. The base pressure in the analysis chamber was in the mid 10^{-11} mbar range, and that in the preparation chamber was in the low 10^{-10} mbar range.

The substrate was a single-crystal rutile TiO_2(110) with dimensions of 10 × 10 × 1 mm (Pi-Kem, Shropshire, UK). This was mounted on a Ta back-plate, ensuring that a good electrical and thermal contact was made. A thermocouple was also attached in close proximity to the crystal to accurately monitor the temperature. Bulk defects were introduced into the crystal by cycles of 2 kV Ar ion sputtering and then annealing at ∼ 700 K until the crystal turned blue. This dopes the crystal n-type[20] and avoids any appreciable sample charging. Heating was achieved by electron beam bombardment of the back of the sample plate.

Before Au deposition the surface was cleaned by 2 kV Ar ion sputtering and checked by observing the disappearance of the C 1s core level signal. To achieve extended flat domains of (110) and to minimize the number of surface defects caused by sputtering, the crystal was annealed at ∼600 K for 10 min.[21] Cooling in oxygen was not undertaken as in previous studies because of the possibility of the formation of surface rosettes.[21] This process was checked by monitoring the shape of the Ti 2p peaks until a single dominant Ti^{4+} oxidation state was observed.

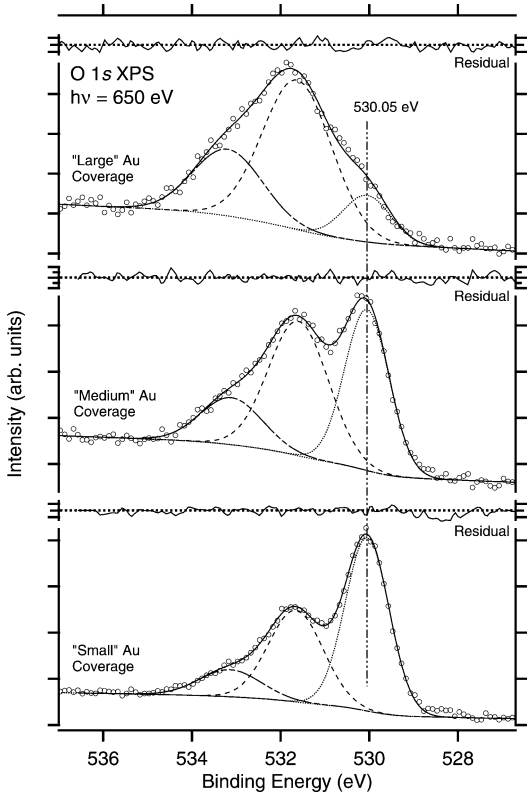

Figure 2. O 1s core level spectra, taken at $h\nu = 600$ eV for the three different Au coverages. Spectra were taken at normal emission. Binding energy is referenced to the substrate signal defined to sit at 530.05 eV.[14] Total instrumentation resolution was ∼240 meV.

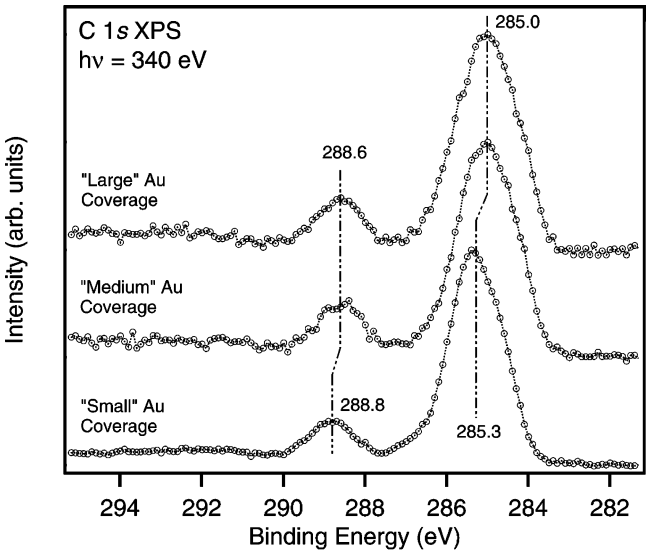

Figure 3. The C 1s core level spectra, taken at $h\nu = 340$ eV for the three different Au coverages. Spectra were taken at normal emission. Binding energy is referenced to the substrate O 1s signal defined to sit at 530.05 eV.[14] Total instrumentation resolution was ∼110 meV.

Gold was evaporated onto the clean surface from a Knudsen cell ∼20 cm from the sample at a temperature ∼1400 K. Three different Au coverages were investigated, denoted as small, medium, and large, indicative of the relative quantities of Au deposited onto the clean surface. These correspond to estimated nominal coverages of <2 monolayers (ML), 3−4 ML, and >5 ML respectively, with associated errors of ∼1 ML. These estimations are based on two measures. The first is the trend in the width of the photoemission onset as compared to studies of Au covered TiO_2(110) made by Howard et al.[24] (it is noted that

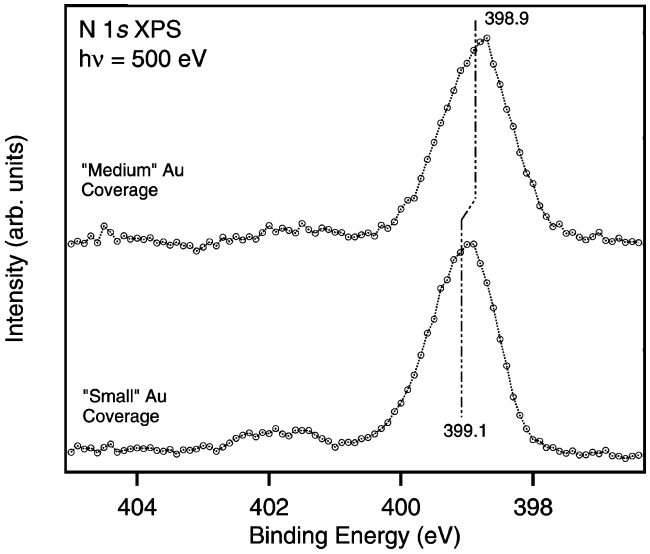

Figure 4. The N 1s core level spectra, taken at $h\nu = 500$ eV for two different Au coverages. Spectra were taken at normal emission. Binding energy is referenced to the substrate O 1s signal defined to sit at 530.05 eV.[14] Total instrumentation resolution was ~190 meV.

differences between experimental resolutions were corrected for). The second measure is the trend in the attenuation of the substrate O 1s core level signal, as fitted by the island growth model developed by Parker et al.[25]

Bi-isonicotinic acid (Sigma-Aldrich, UK) was evaporated onto the Au/TiO_2 from a Knudsen cell ~20 cm from the sample. The powder was outgassed thoroughly and evaporated at a temperature of ~230 °C. Multilayers were made by deposition onto the substrate at room temperature. To achieve ML coverages, a multilayer was first formed and then gently heated off, whereby the physisorbed molecules are lost to leave a chemisorbed monolayer.[13,14] This process was followed in real time by monitoring the shape of the O 1s peaks, which reflect the differing local environments experienced by the two carboxylic oxygen atoms in the two preparations.[11,22] Although thermal damage is a possibility for this monolayer preparation method using a Au(111) substrate, the near-edge X-ray absorption fine structure (NEXAFS) and X-ray photoelectron spectroscopy (XPS) signatures of damage are known[18,23] and did not occur for the results presented here. To further prevent any damage occurring to the molecules from the synchrotron radiation, spectra were recorded while the sample was swept across the beam, ensuring the motion was in the focal plane of the analyzer.

Exit slits of the monochromator were set to give a resolution of ~100 meV for photons of energy $h\nu = 400$ eV. Photon energy calibration was made from the separation between first- and second-order Au 4f peaks. For the recording of NEXAFS and resonant photoemission spectra, a taper (+4 mm) was applied to the undulator to reduce the intensity variation of the radiation as the photon energy was scanned. For these measurements, the analyzer pass energy and entrance slits were set to give an analyzer resolution of ~750 meV and hence a total binding energy resolution of ~760 meV. The analyzer was also set to record spectra in fixed mode. These settings were found to give the best compromise between energy resolution and the large number of counts required for quantitatively analyzable resonant photoemission spectra. For core level spectra, the analyzer was set to give a total energy resolution varying from <120 meV for spectra taken at $h\nu$ <400 eV to ~240 meV at $h\nu = 650$ eV and was set to record in swept mode.

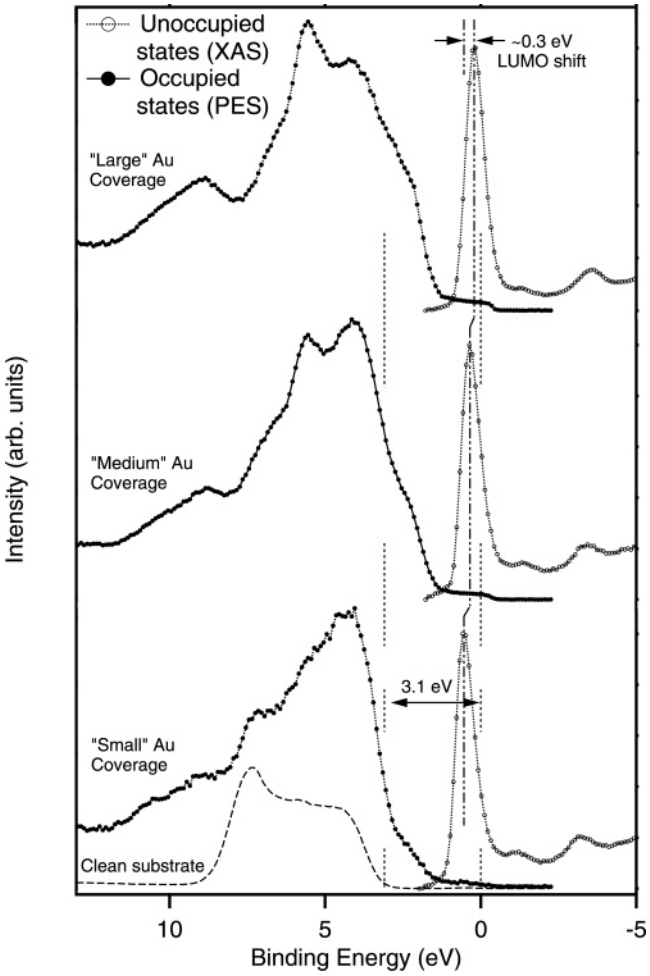

Figure 5. Energy level alignment of substrate and molecular occupied and unoccupied states. Also indicated are the TiO_2 optical band gap of 3.1 eV and the shift of the LUMO resonance (0.3 eV between small and large preparations). The NEXAFS spectrum is over the N 1s edge with PES spectra taken at 110 eV. Spectra were taken at normal emission. Binding energy is referenced to the substrate O 1s signal defined to sit at 530.05 eV.[14] Resolution was better than 110 meV.

All core level and valence band photoemission spectra were calibrated to the substrate O 1s peak at 530.05 eV following previous work of bi-isonicotinic acid adsorbed onto TiO_2-(110).[11,14] To achieve this, the position of the substrate peak was identified from an unconstrained fit of the O 1s spectra of the small Au coverage data set and was shifted to lie at 530.05 eV. This shift was then applied to the O 1s spectra of higher Au-coverage data sets; the substrate components of which were then fitted under the constraint of lying at 530.05 eV. This is justified on the basis of the stability of the beamline and the consistency of other substrate peaks. The beamline stability was confirmed through the position of the sample holder Fermi level that remained constant, within the experimental resolution, throughout the entire experiment. Thus, any peak shifts are because of effects intrinsic to the specific surface preparation, as opposed to changes in experimental conditions. The Ti 2p spectra, which derive solely from substrate atoms, show no relative shifts between the preparations, with the raw spectra overlaying perfectly. It is noted that this is in agreement with Ti 3p spectra in recent studies of $Au/TiO_2(110)$,[9] for Au coverages comparable to those being addressed in this work. This justifies using the substrate peaks as a binding energy reference. In contrast, the binding energy scales for the autoionization spectra are left uncalibrated. A reliable calibration could not be made in these cases because of the small binding

TABLE 1. Parameters for the O 1s Spectra in Figure 2

	small Au coverage (eV)	medium Au coverage (eV)	large Au coverage (eV)
TiO_2 substrate peak (0)	530.05	530.05	530.05
C═O and COO^- peak (1)	531.7	531.6	531.6
OH peak (2)	533.1	533.1	533.2
FWHM 0	1.2	1.2	1.3
FWHM 1	1.4	1.6	1.8
FWHM 2	1.6	1.6	1.8
separation 0−1	1.7	1.6	1.6
separation 1−2	1.4	1.5	1.6

energy window used, which did not capture the Fermi level of the Au clusters or the O 2s signal of the molecule and underlying substrate. The shape of the off resonance valence band could not be used because of the levels of noise present (this signal representing a background in the autoionization spectrum). This does not hamper analysis though. Identification of de-excitation channels in an autoionization spectrum does not require an absolute binding energy scale. Thus, in producing the associated resonant photoemission spectrum, only the photon energy scale must be fully calibrated, as is the case for all results presented in this work.

3. Results

Core level spectra of the bi-isonicotinic acid/Au/TiO_2(110) system for the three different Au coverages (small, medium, and large) were recorded. Figure 2 shows O 1s core level photoemission spectra. These exhibit three distinct peak components. The lowest binding energy (BE) component is identified with the substrate oxygen atoms, as confirmed by its attenuation with increasing quantities of Au, whereas the two higher energy components are identified with the molecular oxygen atoms. Of these latter two components, that at high BE is because of the hydroxyl oxygen (OH) of the intact carboxylic acid group (COOH). That at lower BE has two identities, in that it corresponds both to the carbonyl oxygen (C═O) of the intact carboxylic group (COOH) and to the deprotanted carboxylic (COO^-) form.[11,22] Spectra were fitted with a combination of a linear and a Shirley background followed by three Gaussian peak components. Because of the weak nature of the hydroxyl component of the small Au coverage data, this was constrained to have an upper limit to the full width at half-maximum (FWHM) equal to the FWHM of the corresponding component in the medium Au coverage spectrum (1.6 eV). Finally, the hydroxyl and carbonyl components of the large Au coverage spectrum had a maximum limit to their FWHMs (1.8 eV) to maintain physically realistic components.

These constraints are necessary because of the manifold of possible fits such a broad spectrum can exhibit under the current level of noise, particularly when weak peak components are present. The full set of parameters associated with the O 1s fits are given in Table 1. From the fits it can be seen that, as the quantity of Au increases, the bonding configuration of bi-isonicotinic acid changes.

For the small Au preparation the carbonyl component dominates the molecular peaks. The intensity ratio between the carbonyl and hydroxyl groups reveals that a majority of 65% of the molecular carboxylic groups are deprotonated.[11] Because the surface will be largely TiO_2(110) at this coverage of Au[7,8,10] the molecule can be expected (in the majority case) to bind to the surface in a 2M-bidentate fashion through the carboxylic group, as in previous studies.[11−14]

The effect of the addition of Au is to decrease the relative share of molecules that bind in this 2M-bidentate fashion, as can be seen in the medium and large Au coverage O 1s spectra through the relative growth of the hydroxyl component. For the large Au coverage, the intensity ratio between the carbonyl and hydroxyl peaks shows that a minority of approximately 45% of all molecular carboxylic groups are now deprotonated, with the majority retaining their carboxylic proton. It is noted that it was previously found that bi-isonicotinic acid does not deprotonate when deposited onto Au(111) and that it binds with its ring structure largely aligned with the surface.[18] We will return to this point in the discussion.

Figures 3 and 4 show C 1s and N 1s spectra, respectively, after the removal of an exponential background. Also indicated are the central moments. For the main peak structures these were calculated by fitting the peak with two Gaussians and taking the center of gravity of the pair. The position of the high binding energy C 1s carboxylic peak[14] was determined by fitting with a single Gaussian. The small Au coverage C 1s spectrum agrees well with the study of the molecule on a rutile TiO_2-(110) substrate, with a peak component separation of 3.5 eV as compared to 3.47 eV.[14] In both the C 1s and N 1s cases the medium Au coverage spectra are shifted to lower binding energy as compared to those for the small coverage. No difference exists between the medium and large Au preparation C 1s spectra. It is also noted that preliminary N 1s data for the large coverage also show this. These observations can be rationalized in terms of an increase in the charge screening of the bi-isonicotinic acid molecules by the Au islands. This effect would also be expected to saturate, consistent with the negligible difference between the medium and large Au coverages.

Fundamental in addressing the dynamics of any interfacial charge transfer is the "energetics" of the situation. In the current context this pertains to the energetic positions of the states involved in the passage of charge through the system. This is assessed by the alignment[15] of NEXAFS spectra, which detail the unoccupied molecular states, with valence band photoemission spectra (PES), which provide information on the occupied states. The results for the different Au preparations are presented in Figure 5.

The peak of the LUMO at ∼0.5 eV overlaps with the band gap of the underlying substrate for all preparations. This is as was previously found for bi-isonicotinic acid adsorbed onto TiO_2(110).[15] There is a slight trend of less overlap with increasing Au, with a total shift of the LUMO ∼0.3 eV over the coverages shown, largely mirroring the shifts of the N 1s (and C 1s) spectra. It is noted that the LUMO FWHM does not vary between the preparations, within the experimental resolution. For the small Au coverage, overlap with the substrate band gap is sufficient that no charge transfer out of the LUMO (following resonant excitation) is expected. The same can be said of the medium preparation, but it becomes less certain with the large, where a small amount of charge transfer into the substrate conduction band may be possible from those vibrational levels located at lower binding energy.

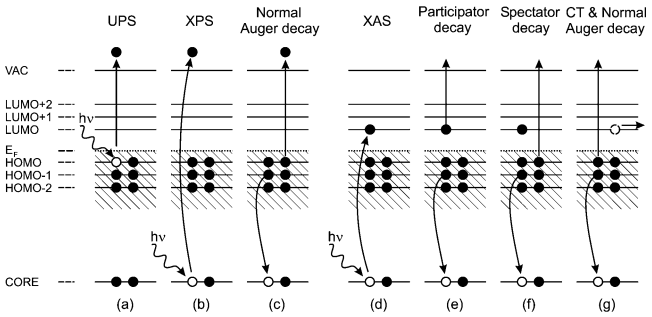

Figure 6. Electron excitation and de-excitation processes. Spheres represent filled and empty discrete molecular states. Hatched areas represent the valence band of an underlying metallic substrate. (a) Valence band photoemission (UPS); (b) core level photoemission (XPS); (c) auger decay following core hole ionization; (d) resonant core level excitation into unoccupied bound states (XAS); (e) participator decay following resonant excitation; (f) spectator decay following resonant excitation; (g) charge transfer out of unoccupied states and subsequent Auger decay, following resonant excitation.

Overlap of the LUMO, in all cases, also occurs with occupied states sitting below (more positive BE) the Fermi level of the Au clusters. It must be remembered that the NEXAFS-derived LUMO is a core-excited state; thus, prior to the initial excitation event, the unoccupied states will actually lie at lower BE as compared to those shown in Figure 5, which reflect the fact that a core hole is present. The magnitude of such a shift can be estimated from the difference between the LUMO BE, as referenced to the vacuum level (through the core level ionization potential), and the electron affinity. It is noted that the polarization of the surroundings has not been taken into account in this estimate. This is justified because screening from electrons in the substrate is not expected to be significant in a bound state transition for which the molecule will remain neutral.[26] For the related molecule of pyridine, this gives an estimate of 5.5 eV,[27] which can be considered as a good approximation to the value for bi-isonicotinic acid. Thus, charge transfer, from occupied states around the Fermi level into unoccupied molecular states, is not expected to occur before core hole creation but can occur, in principle, in the core-excited state.

Assessment of the charge-transfer characteristics of the system was made using the "core hole clock" implementation of resonant photoemission spectroscopy (RPES).[16,17,28−31] This technique is based on the identification of electron emission decay channels following resonant excitation of core level electrons into unoccupied molecular states. In the current work, it is the participator channels that are used. If a strong coupling exists between bi-isonicotinic acid and the surrounding environment, then participator autoionization channels (in the de-excitation process) are modified as compared to the case of an isolated molecule, as electrons transfer out of, or into, unoccupied molecular orbitals. Relevant electron excitation and de-excitation processes are shown in Figure 6. For a complete discussion of the technique, the reader is directed to Brühwiler et al.[30] and the references therein.

Figure 7 shows the autoionization spectra, over the N 1s edge, for the three Au coverages. De-excitation channels sit on a constant, direct photoemission background from valence states (see Figure 6). This background varies between the preparations, with Au valence states becoming more prominent with increasing amounts of Au. The background is relatively strong as a consequence of both the metallic Au clusters and the analyzer position relative to the incoming radiation, which is quite sensitive to the direct PES signal.

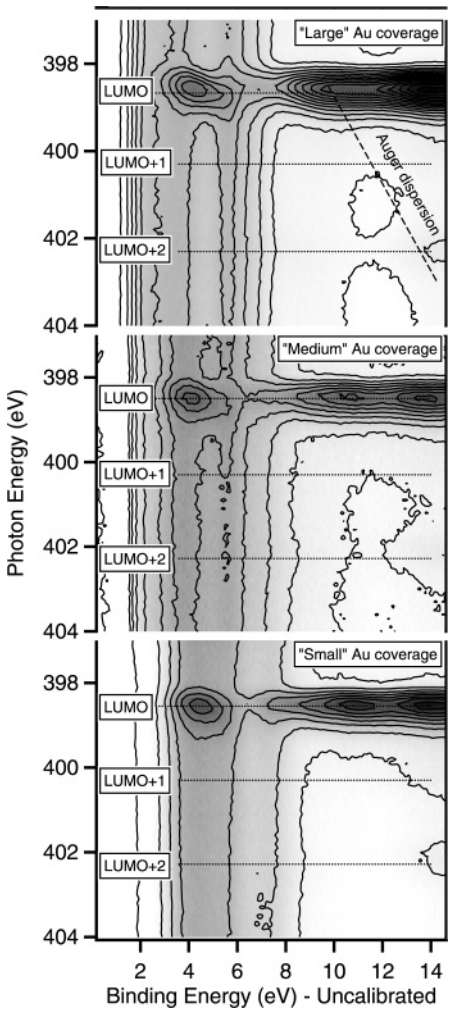

Figure 7. Autoionization spectra over the N 1s edge, for a monolayer of bi-isonicotinic acid on TiO_2(110) containing three different coverages of Au. Indicated are the positions of the LUMO, LUMO + 1 and LUMO + 2. High−low electron counts are indicated as black−white. Contours are derived from smoothed data using a binomial algorithm. Spectra were taken at normal emission. Photon resolution was ∼100 meV, giving a binding energy resolution of ∼760 meV.

Participator and spectator de-excitation channels can be identified by their dispersion behavior. Participator channels will leave the system in an identical final state to valence band photoemission and will therefore disperse linearly with binding energy. By comparison, spectator channels will leave the system in a final state similar to that left by normal Auger decay (following core level ionization). This channel will then disperse linearly with kinetic energy. It is noted that the bandwidth of the photons used in this experiment is large relative to the bandwidth of the electronic energy levels; thus, resonant photoemission is being conducted outside of the Auger Resonant Raman (ARR) regime.[29,30] Operation within this regime was not attempted because the separation between normal Auger and spectator channels is too small to allow a successful identification on the basis of their differing ARR dispersion behavior.

Previous studies of the molecule on TiO_2,[16] as well as unpublished work of our own on the same system, shows that the majority of the participator signal can be captured by a conservative 5 eV window, starting at the onset of the HOMO. No spectator signal enters into this region for these studies. Integration over this window (for each photon energy) gives a resonant photoemission spectrum. For the current system this

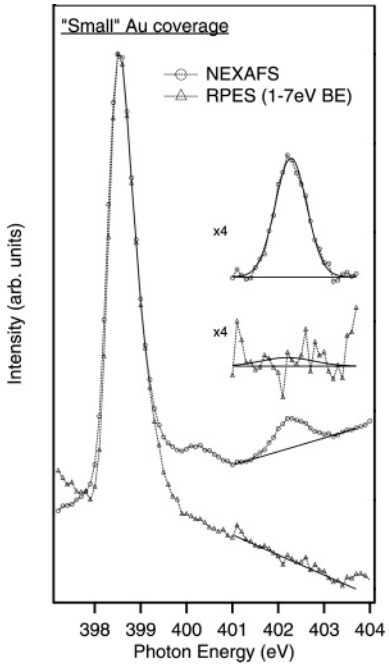

Figure 8. The N 1*s* RPES comparison to NEXAFS (all de-excitation channels) for the small Au preparation. Spectra were vertically shifted to align the low-energy backgrounds and were normalized to the LUMO resonance. The resonant photoemission spectrum was derived by integration of electrons representing binding energies from 1.0−7.0 eV. Spectra were taken at normal emission. Photon energy resolution was ∼100 meV.

window has been extended at the lower binding energy side by 1 eV to include Au-derived states at the top of the valence band.

Figure 8 shows the resonant photoemission and total autoionization channels for the small Au preparation. Normalization of the spectra has been made to the LUMO resonance. Qualitatively, the LUMO + 2 resonance of the participator channel has been suppressed to the level of background noise. This indicates that charge transfer from the molecule to the substrate is occurring. From the energetics (see Figure 5) it must be remembered that charge transfer into the LUMO is possible and could result in an enlarged participator LUMO resonance. Subsequent normalization to such a LUMO would produce a LUMO + 2 that was too weak as compared to the NEXAFS LUMO + 2. However, such an effect is likely to be negligible in the present case because of the relatively small quantities of Au and the large amount of exposed substrate, as can be concluded from the core level spectra.

Denoting the intensity (area) of the LUMO + 2 as I , the charge-transfer time (τ_{CT}) of electrons moving from the LUMO + 2 to substrate states is given by eq 1.[30,17]

$$\tau_{CT} = \tau_{ch} \frac{I^{coup}_{RPES}/I^{coup}_{NEXAFS}}{I^{iso}_{RPES}/I^{iso}_{NEXAFS} - I^{coup}_{RPES}/I^{coup}_{NEXAFS}} \quad (1)$$

The variables I^{iso}_{RPES} and I^{coup}_{RPES} represent the intensities of the participator decay channel as measured in the isolated molecule and coupled molecule−substrate systems, respectively. The time scale τ_{ch} is the average lifetime of an N 1s core hole. This latter quantity has been measured to be 6 fs.[32] Assuming the isolated molecule is well represented by a multilayer preparation, $I^{iso}_{RPES}/I^{iso}_{NEXAFS} = 0.33$.[17] Because no participator LUMO + 2 peak is resolvable in Figure 8, any charge-transfer time is an upper limit (with the proviso of appropriate LUMO normalization). The largest peak reasonably placed in the noise gives $I^{coup}_{RPES}/I^{coup}_{NEXAFS}$ = 0.12. Using eq 1 gives a charge-transfer time of <3 fs, which is in good agreement with the system of bi-isonicotinic acid adsorbed at rutile TiO_2(110).[17,16]

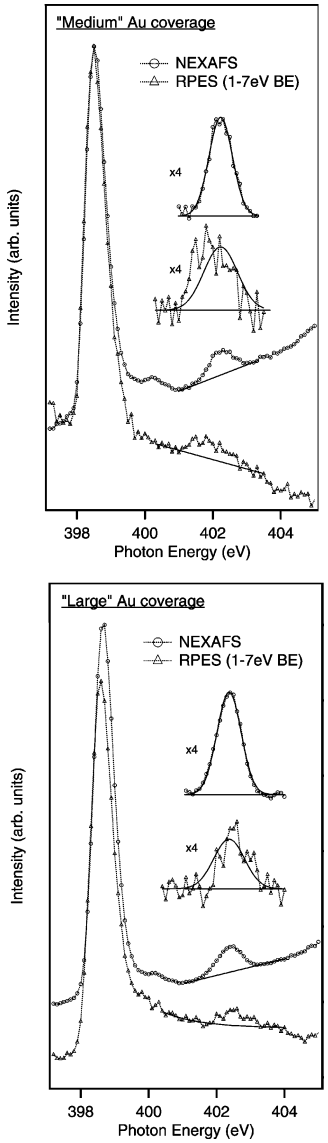

Figure 9. The N 1s RPES comparison to NEXAFS (all de-excitation channels) for the medium and large Au preparation. Spectra were vertically shifted to align the low-energy backgrounds and were normalized to the LUMO resonance. An offset has been applied to the spectra of the large preparation to allow an unhindered comparison. The resonant photoemission spectra were derived by integration of electrons representing binding energies from 1.0−7.0 eV. Spectra were taken at normal emission. Photon energy resolution was ∼100 meV.

It has been shown in experiments for bi-isonicotinic acid on Au(111) that femtosecond charge injection from the molecule to the Au does not occur.[18] It is expected then that, as the coverage of Au is increased for the current system, the participator LUMO + 2 peak should return, reaching a maximum level of ∼0.3 of the LUMO + 2 in the NEXAFS signal.[18] For the higher Au coverages it is indeed found that this peak returns. However, its magnitude is much greater than expected. This is illustrated in Figure 9 for the medium Au preparation. The value of $I^{coup}_{RPES}/I^{coup}_{NEXAFS}$ in this case is 0.9 ± 0.1 (the error in this case is because of the signal-to-noise of the RPES spectra). This was derived by fitting the participator-derived LUMO + 2, following a "background" subtraction, with a Gaussian line shape that was constrained to sit at the energetic position of the NEXAFS-derived LUMO + 2. For the large

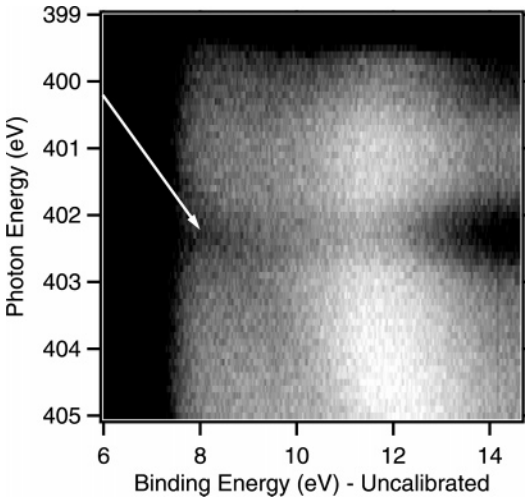

Figure 10. Magnified and contrast adjusted autoionization spectrum over the N 1s edge, for a monolayer of bi-isonicotinic acid on Au/TiO_2(110) for the thick Au preparation. The white arrow indicates the tracking of an Auger feature that lies at a lower binding energy than the normal N 1s Auger. High−low electron counts are indicated as black−white. Spectra were taken at normal emission. Photon resolution was ~100 meV, giving a binding energy resolution of ~760 meV.

Au coverage also shown in Figure 9, this ratio is reduced to a value of 0.6 ± 0.1, although this is still significantly higher than expected.

Although the size of the participator LUMO + 2 in the medium and large preparations is larger than expected, it nevertheless indicates that electrons resonantly excited into the LUMO + 2 remain localized in this orbital on the time scale of the core-hole lifetime. Thus, at least to a large degree, ultrafast charge transfer from the LUMO + 2 to the surroundings does not occur.

The same cannot be said of the reverse situation. There is evidence to suggest that ultrafast back-transfer occurs, from the Au to the bi-isonicotinic acid molecules. The autoionisation spectrum of the large Au preparation shows a weak feature that tracks as an Auger-type signal. This is highlighted in Figure 10 and is most obvious from ($h\nu$ = 402 eV, BE = 8 eV) to ($h\nu$ = 405 eV, BE = 11 eV). This has also been observed, with greater strength, for bi-isonicotinic acid adsorbed onto Au(111),[18] where it was tentatively attributed to ultrafast back-transfer of electrons from Au states into core-excited unoccupied molecular orbitals.

4. Discussion

With sufficient quantities of Au in the bi-isonicotinic acid/Au/TiO_2(110) system, there are three interactions between the molecule and substrate that require consideration: (1) that between the molecule and TiO_2(110) in the absence of Au, (2) that between the molecule and the Au islands in the absence of the substrate, and (3) the combined simultaneous interaction of the molecule with the Au islands and the surface. Competition between these three interactions will be determined by the amount of Au present in the system and is reflected in the photoemission spectra measured. For the extreme cases of zero and infinite Au coverage, the results are well-known from studies of bi-isonicotinic acid/TiO_2(110)[11−17] and bi-isonicotinic acid/Au(111),[18] as has been highlighted previously.

The combined Au and TiO_2 system, in which a considerable fraction of the bare TiO_2 surface is exposed to the vacuum because of the three-dimensional (3D) island growth of the Au overlayer,[7,8,10,9] should be characterized by a mixture of bi-isonicotinic acid adsorption geometries. Clearly, a fraction of the molecules binds in the deprotonated 2M-bidentate geometry characteristic for the bare TiO_2 surface.[11−14] Evidence for this binding mode is found from the O 1s spectra for all three investigated Au coverages, as shown above. Those molecules that only interact with the Au cluster surface are expected to remain protonated as on Au(111)[18] and thus give rise to a large part of the hydroxyl peak in the O 1s spectra. Moreover, the superposition of the spectral peaks from these two different chemical environments should lead to an increase in the width of the energy levels because of a larger manifold of binding energies realized. Such an increase is seen quantitatively in the FWHM of the O 1s spectra as well as qualitatively in the C 1s and N 1s spectra. The most interesting question is whether there exists a third binding mode at the significant number of Au−TiO_2 phase boundaries, which would give rise to a further broadening of the spectral features.

A more quantitative analysis of the core-level spectra provides further insight into the binding of bi-isonicotinic acid to the mixed Au/TiO_2 surface. Beginning with the O 1s spectra, we first note that good fits are obtained using three peak components, the resolution of the data does not justify the inclusion of more. Thus, the variation in the signals from molecules in different environments will, in general, be reflected in both the positions and the FWHM of these components. It is observed that the O 1s peak positions are affected by the differing Au coverages only to a limited amount; the peaks shift by not more than 0.1 eV throughout the series. Such relatively static positions means that only a limited amount of variation in the FWHM is attainable through a changing superposition of only two components, namely, those originating from the molecule interacting with Au and the molecule interacting with the TiO_2 substrate. However, FWHMs are observed to increase significantly for increasing coverage. Thus, to be consistent with trends in both peak positions and FWHMs, at least one further type of interaction must be present.

Further issue with the trend in the FWHMs exists. That the FWHMs should increase as the size of Au clusters increase is somewhat counter-intuitive to the notion that the spectral signatures of bi-isonicotinic acid bonded to TiO_2(110) in a 2M-bidentate fashion and bi-isonicotinic acid bonded to Au superpose to exhibit the spectrum observed for the mixed system. In particular, an increase of the Au cluster size when going from the small to the large Au coverage would be expected to lead to a smaller variation in adsorbate geometry on the available Au surface and, hence, to a smaller variation in binding energy.

Thus, we speculate that there exists a third kind of bonding situation that increases in significance for larger cluster sizes and that would provide another contribution to the spectral appearance of the mixed sample. This third kind of adsorbate geometry is thought to occur at the Au/TiO_2 phase boundaries and to be characterized by a bond between a nondeprotonated carboxylic functional group and the TiO_2 substrate, that is, by the formation of a bond between the carbonyl and the substrate Ti atoms. This bond is hinted at by the energetic position of the carbonyl peak component, suggesting that the chemical environment of the carbonyl oxygen is energetically similar in the cases where the molecule has and has not deprotonated. Also instructive in this regard is a comparison of the separation of the carbonyl and hydroxyl peaks for all three preparations (1.4−1.6 eV) to those found for a bi-isonicotinic acid multilayer (1.23 eV)[14] and bi-isonicotinic acid adsorbed on Au(111) (1.42 eV).[18] The peak separation observed here is significantly larger than for the multilayer and is comparable to (small Au coverage) or larger than (medium and large Au coverages) that found in

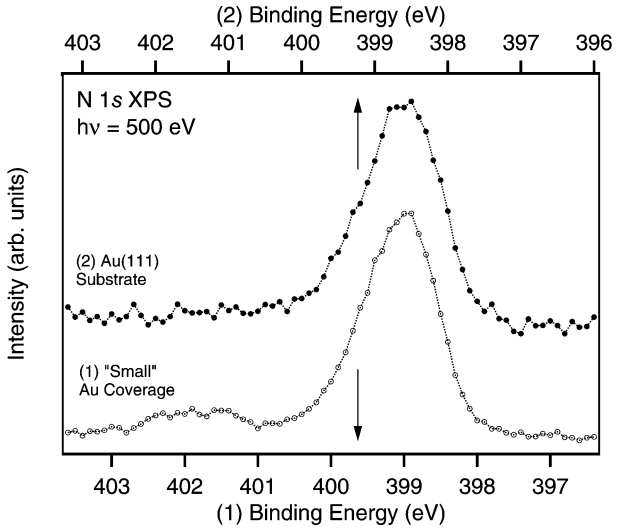

Figure 11. The N 1s core level spectra taken at $h\nu = 500$ eV for bi-isonicotinic acid/Au/TiO_2(110) for the small Au preparation and for bi-isonicotinic acid/Au(111). Spectra were taken at normal emission. Binding energy for the small Au preparation is referenced to the substrate O 1s signal defined to sit at 530.05 eV,[14] whereas the binding energy for the Au(111) spectrum is referenced to the Fermi level of the substrate. Total instrumentation resolution was ~190 meV.

the Au(111) case. It is also seen that the substrate−carbonyl peak separation for all three preparations is in good agreement with that measured for bi-isonicotinic acid on TiO_2(110) (1.65 eV).[14]

Such a bond is unlikely for the case in which the adsorbate has the possibility of deprotonating. However, if the Au clusters cover the substrate reaction partners in the deprotonation reaction, then this possibility is effectively excluded. The exact mechanism of this reaction is not known, but it is likely to involve bridging oxygen atoms. Indeed, the bridging oxygen atoms, as well as the bridging oxygen vacancies, have been found to be preferential adsorption sites for the Au atoms/clusters.[8,9,33] It is also fair to assume that an increasing Au coverage leads to an increasing number of substrate binding sites that lack deprotonation reaction partners; hence, the observed change in FWHMs as a function of cluster size could be explained by this model. It is interesting to note that these clusters could not only be responsible for preventing the deprotonation but they also could act as van der Waals partners for the bipyridine ring of the carbonyl bonded bi-isonicotinic acid.

To further substantiate our speculations, we would like to remark that large O 1s peak separations have been observed in the related system of fluorescein bonded to TiO_2(110), where the increase was attributed to a possible interaction of a carbonyl group with the surface.[22] Furthermore, as stated previously, for the case of bi-isonicotinic acid on Au(111), the carbonyl−hydroxyl peak separation was found to be greater than for multilayers of the molecules, which was attributed to a reduction in binding energy of the carbonyl oxygen through interaction with the surface.[18] These observations go along well with the variations in peak separation discussed above.

Now turning to the C 1s and N 1s spectra, these support an interaction between the pyridine ring structure and the gold islands, through a shift to lower binding energy with increasing Au. A somewhat more subtle effect is the reduction in the intensity of the N 1s shakeup, located at ~402 eV. A comparison between N 1s spectra for the small preparation and the molecule on Au(111) is made in Figure 11, from which it can be seen the shakeup disappears when the molecule is adsorbed onto Au(111). The shakeup is assumed to derive from inter-ring charge redistribution[34] along the lines of that observed in biphenyl.[35] The disappearance/intensity reduction of the shakeup is then explained by perturbation of the molecular orbitals, which breaks the assumed conjugation between the orbitals of the two ring structures.[35]

The most striking result of the combined bi-isonicotinic acid/Au/TiO_2 system is the growth of the participator LUMO + 2 resonance when comparing the medium to the small Au preparation. That no such resonance is observed for the small preparation is unsurprising on the basis of the core level spectra. These reveal that the system is highly similar to that of bi-isonicotinic acid/TiO_2, with the majority of molecules deprotonated and, thus, presumably bound to the TiO_2 surface in a 2M-bidentate geometry.[14] Hence, ultrafast charge transfer is expected to proceed in the majority case with no appreciable resonant enhancement of states from participator channels. However, the appearance of the participator LUMO + 2 for the medium Au preparation, implying that ultrafast charge transfer has been blocked, is surprising on the basis of the O 1s spectra this coverage exhibits. From the component ratios there are still a relatively large number (over half) of carboxylic groups that have deprotonated. Such groups will be chemically reactive and are known to form a chemical bond with the TiO_2 substrate.[11,13,14] Even if the substrate were inaccessible, such functional groups would bind to the Au clusters. Thus, in each case, the condition of significant wavefunction mixing between the molecule and its surroundings, required for ultrafast charge transfer, is likely to be fulfilled.

The apparent discrepancy between the appearance of the participator LUMO + 2 and the number of deprotonated molecular carboxylic groups is rationalized through the fact that the participator LUMO + 2 need not originate from all molecules, only those that are weakly bound to the surroundings. It is proposed that ultrafast charge transfer still occurs from those deprotonated molecules and that the participator LUMO + 2 signal is only due to those molecules whose carboxylic groups remain protonated.

That not all molecules produce the participator LUMO + 2 signal is also made feasible by the fact that the signal is larger than the expected maximum signal[16,18] (~0.3 of the corresponding NEXAFS signal in the absence of charge transfer). By this it is meant that even if all molecules were to contribute, the size of the peak could not be explained. This is also true for the large Au coverage for which resonant photoemission spectra show a larger than expected participator LUMO + 2 resonance. It should be noted that incorrect normalization of the spectra cannot account for this result. In considering the energetics of the systems, the maximum of the LUMO resonance to which normalization is made lies well within both the substrate band gap and the occupied states of the Au clusters. Thus, only the possibility of charge transfer into the LUMO needs to be considered with respect to the normalization procedure. Such a process could only act to make the LUMO larger, which would cause the relative intensity of the LUMO + 2 to be reduced in comparison. By this argument, the large size of the participator LUMO + 2 must be real because the participator LUMO + 2 resonance is a lower estimate at worst.

To create a participator LUMO + 2 resonance larger than that of both the molecule on Au(111)[18] and the multilayers of the molecule,[16] some perturbation to molecular orbitals must exist in the absence of any calibration errors (specifically the assumption that no charge transfers out of the LUMO reso-

nance). Changes to the highest occupied molecular orbitals of the molecule are implied by the loss of the N 1s shakeup feature as the Au coverage is increased. However, any changes in the molecular valence band region are masked by the dominating nature of the Au 5d states. No obvious changes in the density of states of the (core-excited) unoccupied molecular orbitals are observed between the preparations or in comparison to previous studies.[13,18] This would suggest that appreciable orbital changes do not occur to the unoccupied states, thereby lending weight to changes primarily in the occupied states. However, these are energetic positions, so this does not preclude the possibility of some spatial changes.

Any perturbation of molecular orbitals is reflected in the resonant photoelectron spectra through the Auger decay matrix element. This matrix element has been evoked in previous work[16] to motivate the difference in intensities between the NEXAFS-derived and RPES-derived LUMO + 2 resonances in a multilayer preparation of bi-isonicotinic acid on TiO_2 for which no charge transfer was expected.

The Auger decay matrix element (M) influences the intensity of resonances through the Auger transition rate that is given by a Fermi's Golden Rule treatment of the transitions. For a system where no charge transfer can occur, following normalization to the LUMO resonance the intensity $I(\mathrm{LUMO}+2)^{\mathrm{iso}}_{\mathrm{RPES}}/I(\mathrm{LUMO}+2)^{\mathrm{iso}}_{\mathrm{NEXAFS}}$ will be reflected by the participator matrix elements $M(\mathrm{LUMO}+2)_{\mathrm{RPES}}/M(\mathrm{LUMO})_{\mathrm{RPES}}$. An increase in the participator LUMO + 2 can then occur through an increase in $M(\mathrm{LUMO}+2)_{\mathrm{RPES}}$ or a decrease in $M(\mathrm{LUMO})_{\mathrm{RPES}}$.

The matrix elements are dependent upon the Coulomb operator-modified overlap between the initial and final state wavefunctions of the system. Assuming the applicability of single electron states, this takes the form $\langle\phi^*_{\mathrm{Occ}}\,\phi^*_k|1/r|\phi_{\mathrm{N1s}}\phi_{\mathrm{Unocc}}\rangle$, where ϕ_{Occ} represents the state of a hole in the occupied orbitals of the low BE region of the valence band that are involved in participator decay, ϕ_k is the electron emitted, ϕ_{N1s} represents the state due to the core-hole, and ϕ_{Unocc} represents the core-excited unoccupied state (i.e., LUMO, LUMO + 1, etc.). An increase in $M(\mathrm{LUMO}+2)_{\mathrm{RPES}}$ would then be motivated by a decrease in the spatial extent of the LUMO + 2 or the low BE valence states, yielding a smaller spatial separation between these orbitals, which feature in the initial- and final-state wavefunctions. Similarly, a decrease in $M(\mathrm{LUMO})_{\mathrm{RPES}}$ would be motivated by an increase in the spatial extent of the LUMO or the low BE valence states. It is noted that matrix elements associated with the NEXAFS signal have not been considered. These are neglected on the basis that many more states contribute to the intensity of this signal; hence, changes to the top of the valence band are much less important as compared to the affect on the participator signal. It is stressed that the matrix element arguments presented are plausible suppositions only and that resolution of the problem requires a detailed theoretical analysis through computational methods.

Interestingly, the participator LUMO + 2 is largest for the medium Au case. This would suggest that increasing the levels of Au beyond the medium coverage results in the system tending to that of bi-isonicotinic acid on Au(111), for which $I^{\mathrm{coup}}_{\mathrm{RPES}}/I^{\mathrm{coup}}_{\mathrm{NEXAFS}}$ is $\sim$0.3.[18] The normalization procedure could explain this trend. For the large preparation more Au exists and as such, provided charge transfer on the time scale of the core hole into the LUMO does occur, the participator LUMO resonance would increase in comparison to the LUMO + 2. Subsequent normalization would then yield a smaller participator LUMO + 2.

Ultrafast charge transfer from the Au into the molecule would appear to be occurring on the basis of the consistent explanation of the Auger feature, highlighted in Figure 10. Importantly, in a study of the molecule on Au(111),[18] the feature was not observed for multilayers of the molecule nor for the clean Au(111) substrate, showing it derived from an interaction between the molecule and the Au. It was suggested that the feature resulted from ultrafast charge transfer from substrate states located at the Fermi level and into energetically overlapping LUMO states of the (core-excited) molecule. This explains both the narrow BE width of the feature and its appearance at a lower BE than the normal N Auger (because it involves occupied LUMO states) and by an amount comparable to the separation of the molecule-derived HOMO and LUMO states. Accordingly, this feature is defined here as a super-spectator. It is worth noting that such transfer does not necessitate a bond between the molecule and the Au. It has been shown for Ar separated from a Ru(001) substrate by an atomic Xe spacer layer that charge transfer away from resonantly excited Ar occurs on a time scale of 12 fs.[29]

Evidence for ultrafast back-transfer should also exist in the creation of a new participator decay channel.[30] This arises from participator decay in the presence of a second electron that has transferred into the unoccupied orbitals from the substrate, in response to core-hole creation. Thus, the channel will be shifted because of the screening properties of this second electron. However, no evidence of two participator peaks in the resonant photoemission spectra has been found. This is unsurprising though, because the signal would be both small and not far shifted from the "usual" participator signal, making its resolution extremely difficult.

Irrespective of the last point, it is important to realize that the assertion of back-transfer from Au states must be treated with more caution than the forward transfer. Consider an electron passing from molecular states to Au states. This electron will delocalize, existing in a mixed state where it will coherently sample all coupled states. Because of the enormous number of conduction band states, this significantly lengthens the recurrence of the electron on the molecular state. Moreover, coherence with the initial state is lost on a time scale on the order of 10 fs through electron relaxation processes.[36,37] Thus, the continuum of states is sufficient to localize the electron in the substrate. This is in contrast to the reverse situation where charge is transferred from a continuum of states into a discrete molecular state. Charge localization on the molecule requires the breaking of the energy level alignment by nuclear degrees of freedom. This takes on the order of 100 fs for most molecular species.[36,37] In going from molecule to substrate, it is the electron relaxation that determines an upper limit to the charge-transfer time (assuming sufficient electronic coupling). Upon going from substrate to molecule, the nuclear coordinate determines the upper limit on the transfer time.

Evidence for nuclear degrees of freedom of bi-isonicotinic acid operating on a femtosecond time scale can be found in Figure 7. The "twist" exhibited in the LUMO participator resonance can be attributed to vibronic coupling effects along the lines of Schiessling et al.[38] That vibronic coupling effects should appear reveals intramolecular rearrangements occurring on the time scale of the core hole, supporting the possibility of ultrafast back-transfer.

5. Conclusion

For bi-isonicotinic acid/Au/TiO_2(110), where the Au coverage is nominally $<2 \pm 1$ ML, the system behaves largely as it would

in the absence of the Au. This is concluded from core level and resonant photoemission spectra as compared to studies of the molecule on TiO_2.[11,14,16] In these cases, the molecule largely exhibits deprotonation of the carboxylic groups upon surface adsorption and allows the transfer of charge to the substrate on a <3 fs time scale, following resonant excitation of a N 1s core level electron into unoccupied states. The addition of further quantities of Au changes the bonding characteristics of the molecule. This is particularly reflected in the O 1s core level spectra, which show the molecule is more prone to retain the proton associated with the carboxylic group. This is in line with studies of the molecule on Au(111), for which the same behavior is observed. The most dramatic change the Au makes, for nominal coverages of only $3-4 \pm 1$ ML, is in the larger-than-expected increase in the intensity of the participator-derived LUMO + 2 in comparison to the NEXAFS-derived LUMO + 2. It is suggested that this stems from a change in the Auger decay matrix element for the de-excitation process. Although the intensity increase is not accounted for, it is reasonable to suspect that femtosecond charge transfer is not occurring for those molecules that have protonated carboxylic groups. However, there is also evidence to suggest that ultrafast back-transfer from Au to the molecule does occur. This was derived from a narrow Auger feature, at a shallower BE as compared to the main N Auger, in the autoionization spectrum of the $>5 \pm 1$ ML Au coverage. This same super-spectator feature is observed for the system bi-isonicotinic acid/Au(111)[18] and represents an interaction of the molecule with the Au. The implications of these results in the context of solid-state dye-sensitized solar cells are significant. Charge injection from the molecule to the TiO_2(110) substrate occurs on the low femtosecond time scale, but an additional layer of gold between the molecule and the oxide suppresses ultrafast injection by a modification of the adsorption bonding. At the same time, ultrafast back-donation from the gold to the molecule may offer an efficient route to replenish electrons lost from the molecule. These two seemingly mutually exclusive effects can, in principle, be combined in a molecule that could simultaneously bind to both the oxide and intermediate amounts of gold through different ligands.

Acknowledgment. We are grateful for financial support by the European Community - Research Infrastructure Action under the FP6 "Structuring the European Research Area" Programme (through the Integrated Infrastructure Initiative "Integrating Activity on Synchrotron and Free Electron Laser Science"), the UK Engineering and Physical Sciences Research Council (EPSRC), and Vetenskapsrådet. We also wish to give thanks to the staff of MAX-lab for technical assistance.

References and Notes

(1) Grätzel, M. *Nature* **2001**, *414*, 338.
(2) Grätzel, M.; O'Regan, B. *Nature* **1991**, *353*, 737.
(3) Hagfeldt, A.; Grätzel, M. *Acc. Chem. Res.* **2000**, *33*, 269.
(4) McFarland, E. W.; Tang, J. *Nature* **2003**, *421*, 616.
(5) Grätzel, M. *Nature* **2003**, *421*, 586.
(6) Seah, M. P.; Dench, W. A. *Surf. Interface Anal.* **1979**, *1*, 2.
(7) Zhang, L.; Persaud, R.; Madey, T. E. *Phys. Rev. B* **1997**, *56*, 10549.
(8) Minato, T.; Susaki, T.; Shiraki, S.; Kato, H. S.; Kawai, M.; Aika, K. *Surf. Sci.* **2004**, *566−568*, 1012.
(9) Okazawa, T.; Kohyama, M.; Kido, Y. *Surf. Sci.* **2006**, *600*, 4430.
(10) Koole, R.; Liljeroth, P.; Oosterhout, S.; Vanmaekelbergh, D. *J. Phys. Chem. B* **2005**, *109*, 9205.
(11) Patthey, L.; Rensmo, H.; Persson, P.; Westermark, K.; Vayssieres, L.; Stashans, A.; Petersson, Å.; Brühwiler, P. A.; Siegbahn, H.; Lunell, S.; Mårtensson, N. *J. Chem. Phys.* **1999**, *110*, 5913.
(12) Persson, P.; Lunell, S.; Brühwiler, P. A.; Schnadt, J.; Södergren, S.; O'Shea, J. N.; Karis, O.; Siegbahn, H.; Mårtensson, N.; Bässler, M.; Patthey, L. *J. Chem. Phys.* **2000**, *112*, 3945.
(13) Schnadt, J.; Schiessling, J.; O'Shea, J. N.; Gray, S. M.; Patthey, L.; Johansson, M. K. J.; Shi, M.; Krempaský, J.; Åhlund, J.; Karlsson, P. G.; Persson, P.; Mårtensson, N.; Brühwiler, P. A. *Surf. Sci.* **2003**, *540*, 39.
(14) Schnadt, J.; O'Shea, J. N.; Patthey, L.; Schiessling, J.; Krempaský, J.; Shi, M.; Mårtensson, N.; Brühwiler, P. A. *Surf. Sci.* **2003**, *544*, 74.
(15) Schnadt, J.; O'Shea, J. N.; Patthey, L.; Krempaský, J.; Mårtensson, N.; Brühwiler, P. A. *Phys. Rev. B* **2003**, *67*, 235420.
(16) Schnadt, J.; O'Shea, J. N.; Patthey, L.; Kjeldgaard, L.; Åhlund, J.; Nilson, K.; Schiessling, J.; Krempaský, J.; Shi, M.; Karis, O.; Glover, C.; Siegbahn, H.; Mårtensson, N.; Brühwiler, P. A. *J. Chem. Phys.* **2003**, *119*, 12462.
(17) Schnadt, J.; Brühwiler, P. A.; Patthey, L.; O'Shea, J. N.; Södergren, S.; Odelius, M.; Ahuja, R.; Karis, O.; Bässler, M.; Persson, P.; Siegbahn, H.; Lunell, S.; Mårtensson, N. *Nature* **2002**, *418*, 620.
(18) Taylor, J. B.; Mayor, L. C.; Swarbrick, J. C.; O'Shea, J. N.; Isvoranu, C.; Schnadt, J. *J. Chem. Phys.*, *127*, in press.
(19) Nyholm, R.; Andersen, J. N.; Johansson, U.; Jensen, B. N.; Lindau, I. *Nucl. Instrum. Methods Phys. Res., Sect. B* **2001**, *467−468*, 520.
(20) Diebold, U. *Surf. Sci. Rep.* **2003**, *48*, 53.
(21) Li, M.; Hebenstreit, W.; Gross, L.; Diebold, U.; Henderson, M. A.; Jennison, D. R.; Schultz, P. A.; Sears, M. P. *Surf. Sci.* **1999**, *437*, 173.
(22) O'Shea, J. N.; Taylor, J. B.; Smith, E. A. *Surf. Sci.* **2004**, *548*, 317.
(23) Taylor, J. B.; Mayor, L. C.; Swarbrick, J. C.; O'Shea, J. N.; Schnadt, J. 2006, unpublished results.
(24) Howard, A.; Clark, D. N. S.; Mitchell, C. E. J.; Egdell, R. G.; Dhanak, V. R. *Surf. Sci.* **2002**, *518*, 210.
(25) Parker, S. C.; Grant, A. W.; Bondzie, V. A.; Campbell, C. T. *Surf. Sci*. **1999**, *441*, 10.
(26) Stöhr, J. *NEXAFS Spectroscopy*; Springer: Berlin, 1992.
(27) Schnadt, J.; Schiessling, J.; Brühwiler, P. A. *Chem. Phys.* **2005**, *312*, 39.
(28) Björneholm, O.; Nilsson, A.; Sandell, A.; Hernnäs, B.; Mårtensson, N. *Phys. Rev. Lett.* **1992**, *68*, 1892.
(29) Wurth, W.; Menzel, D. *Chem. Phys.* **2000**, *251*, 141.
(30) Brühwiler, P. A.; Karis, O.; Mårtensson, N. *Rev. Mod. Phys.* **2002**, *74*, 703.
(31) Föhlisch, A.; Feulner, P.; Hennies, F.; Fink, A.; Menzel, D.; Sanchez-Portal, D.; Echenique, P.; Wurth, W. *Nature* **2005**, *436*, 373.
(32) Kempgens, B.; Kivimäki, A.; Neeb, M.; Köppe, H. M.; Bradshaw, A. M.; Feldhaus, J. *J. Phys. B* **1996**, *29*, 5389.
(33) Matthey, D.; Wang, J. G.; Wendt, S.; Matthiesen, J.; Schaub, R.; Lægsgaard, E.; Hammer, B.; Besenbacher, F. *Science* **2007**, *315*, 1692.
(34) Schnadt, J.; Henningsson, A.; Andersson, M. P.; Karlsson, P. G.; Uvdal, P.; Siegbahn, H.; Brühwiler, P. A.; Sandell, A. *J. Phys. Chem. B* **2004**, *108*, 3114.
(35) Enkvist, C.; Lunell, S.; Svensson, S. *Chem. Phys*. **1997**, *214*, 123.
(36) Lanzafame, J. M.; Palese, S.; Wang, D.; Miller, R. J. D.; Muenter, A. A. *J. Phys. Chem.* **1994**, *98*, 11020.
(37) Lanzafame, J. M.; Miller, R. J. D.; Muenter, A. A.; Parkinson, B. A. *J. Phys. Chem*. **1992**, *96*, 2820.
(38) Kjeldgaard, L.; Käämbre, T.; Schiessling, J.; Marenne, I.; O'Shea, J. N.; Schnadt, J.; Glover, C. J.; Nagasono, M.; Nordlund, D.; Garnier, M. G.; Qian, L.; Rubensson, J. E.; Rudolf, P.; Mårtensson, N.; Nordgren, J.; Brühwiler, P. A. *Phys. Rev. B* **2005**, *72*, 205414.